

# Morphological and optical properties of ultra-thin nanostructured Cu films deposited by RF sputtering on nanoporous anodic alumina substrate

Mohamed Shaban<sup>1</sup> ✉, Ashour M. Ahmed<sup>1</sup>, Ehab Abdel- Rahman<sup>2</sup>, Hany Hamdy<sup>1</sup>

<sup>1</sup>Nanophotonics and Applications Lab, Department of physics, Faculty of Science, Beni-Suef University, Beni-Suef 62514, Egypt

<sup>2</sup>Yousef Jameel Science and Technology Research Center, American University in Cairo, New Cairo, Cairo 11835, Egypt  
✉ E-mail: mssfadel@yahoo.com

Published in Micro & Nano Letters; Received on 23rd December 2015; Revised on 22nd March 2016; Accepted on 23rd March 2016

Nanoporous materials have attracted considerable technological interest due to their wide range of applications. In this study, highly ordered nanoporous anodic alumina substrates (NAAS) were fabricated by two-steps anodisation. Radio-frequency (RF) magnetron sputtering was used to deposit ultrathin Cu layers of different morphologies on the top surface of NAAS. From the field emission-scanning electron microscope images, the Cu/NAAS morphologies were tuned from nanoporous ultra-thin Cu layer, to nanoporous-grains of Cu aggregates, then to a continuous layer of Cu nanostones as the deposition time increased from 1 to 4 min. The reflection spectra of the Cu/NAAS samples were dominated with localised surface plasmon modes; longitudinal, transverse and higher-order modes. The surface plasmon resonances of the fundamental and higher-order longitudinal modes were shifted to longer wavelengths as the deposition time increased. In addition, the transverse surface plasmon resonances were shifted to longer wavelengths for deposition time  $\leq 3$  min (nanoporous Cu film) and suddenly shifted to shorter wavelengths for deposition time  $\geq 4$  min (continuous film). The correlations between the structural parameters and the shift of surface plasmon resonance modes were discussed. The strong red-shifted of the surface plasmon modes to the NIR region suggests a unique opportunity for the design of biomedical sensor based on the proposed structures.

**1. Introduction:** Metal nanostructures are widely used in many technological applications ranging from photonics to biotechnology due to their unique optical properties from localised surface plasmon resonance. The localised surface plasmon resonance (SPR) is excited when the free conduction electrons within the nanoparticles are induced to coherent oscillation by interacting electromagnetic fields of light [1]. This localised SPR is characterised by substantial enhancements of the local electric fields surrounding the nanoparticles [2]. Many metals such as silver, platinum, and gold are widely used to support SPR [3–5]. However, there is strong demand for cheap and reliable plasmonic materials to replace the expensive plasmonic nanostructures such as Au and Ag. From many ways, Cu is one of the best options for different reasons such as it permits plasmonic excitation in the visible and NIR regions, its low price, and its relative abundance on earth is higher than Ag, Au, and Pt. Moreover, copper has low electrical resistivity, high electromigration resistance and excellent catalytic property [6]. Hence, it has been used in different applications such as sensors, electronics, solar energy transformation, surface-enhanced Raman scattering, and catalysts [7–12].

However, there is a few number of researchers focus on fabrication and characterisation of Cu nanoarrays that can be support localised SPR. Duan *et al.* [13] studied the SPRs of Cu nanowire arrays deposited by electrochemical deposition on polycarbonate membranes. In this study, two transverse SPRs were obtained at 540 and 563 nm. However, irregular distribution of the nanowires, low controllability of the distances between them, and small filling factor result in weak and broadened SPRs. George *et al.* [14] studied the effect of oxidation on localised SPR of the Cu nanoparticles arrays that fabricated by nanosphere lithography. Lithography technology has some disadvantages that may limit their applications in manufacturing such as it is expensive and long-time consumption [15]. Yaya *et al.* [16] studied the effect of temperature on the SPR of Cu nanowire arrays deposited inside the pore of nanoporous anodic alumina substrates (NAAS). Two wide broadened SPRs were obtained at 585 and 1808 nm.

However, the morphologies of the Cu/NAAS structures were not addressed in this study. From the previous discussion, most of the previous studies have many drawbacks and a new strategy is strongly required to deposit Cu nanoarrays in/on the nanoporous templates with reliable and inexpensive technology. Radio-frequency (RF) magnetron sputtering has received considerable attention because of its advantages such as easy control, high efficiency, and suitable for large-scale film deposition. For many applications such as sensors and catalysts, depositing metallic nanostructures on the outer surface of the NAAS will be more beneficial. These due to the nanostructures on the outer surface of the NAAS have a higher opportunity of touching the reactant than those inside. Also, the large surface area of porous NAAS enhances the reactivity of NAAS with various chemical species. The present study reports the fabrication and characterisation of Cu nanoarrays on the top surface of the NAAS by the RF magnetron sputtering.

**2. Materials and methods:** The NAAS was prepared by a two-step electrochemical anodisation process of high-purity aluminium foils (99.99%) [17, 18]. The first-step anodisation was performed in a 0.3 M  $C_2H_2O_4$  solution under an anodising voltage of 40 V for 4 h at 10°C. To improve the uniformity of the pores, the generated alumina during the first anodisation was removed in a mixture of  $H_3PO_4$  and  $CrO_3$ . A second anodisation was performed for 6 min by applying the same parameters as in the first anodisation. Finally, the pores were widened and the barrier layer was dissolved by isotropic chemical etching in  $H_3PO_4$  for 45 min at room temperature. Ultra-thin Cu films were deposited on the NAAS surface by radio-frequency magnetron sputtering using a circular Cu target (purity, 99.99%). The sputtering time was varied from 1 to 4 min to obtain various film thicknesses.

The morphologies and chemical composition of the as-prepared and the Cu/ films were studied using field emission-scanning electron microscope (model: ZEISS SUPRA 55 VP and ZEISS LEO, Gemini Column) equipped with an energy-dispersive X-ray spectroscopy (EDX). Optical studies of the samples were performed by measuring the reflectance spectra using UV-VIS-IR

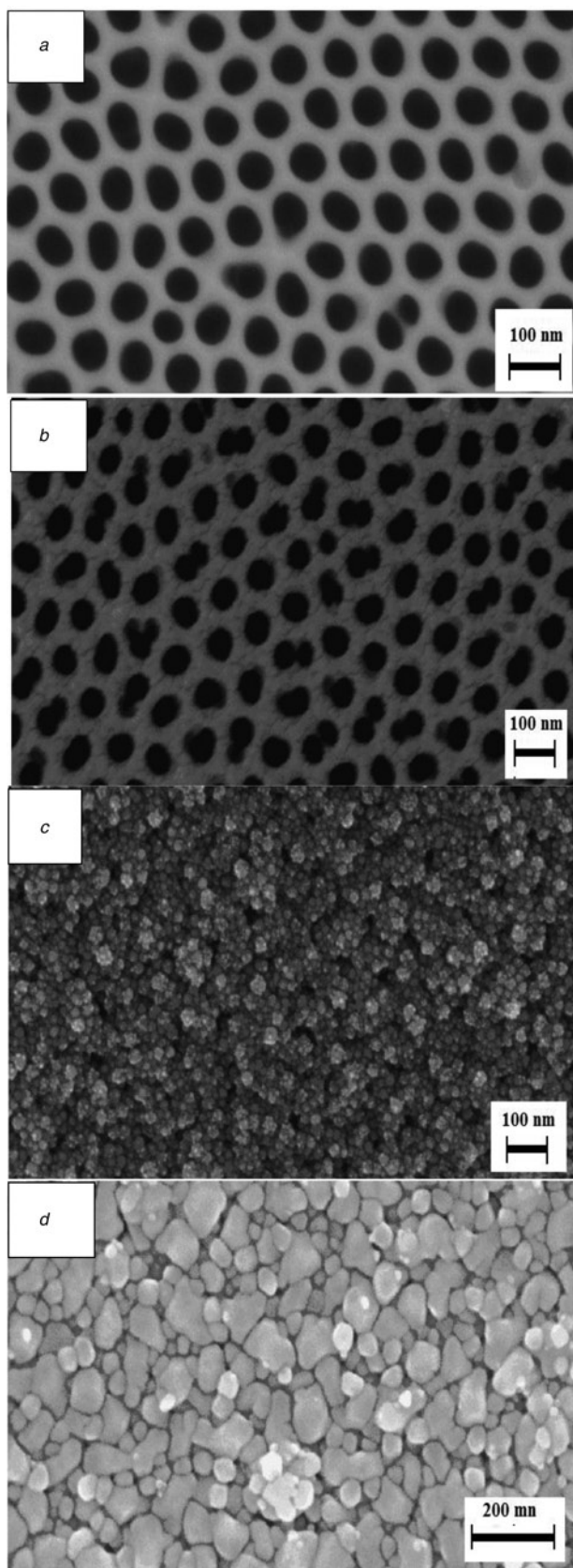


**Fig. 1** SEM images of  
*a* Pore widened NAAS and NAASs coated with Cu for  
*b* 1 min  
*c* 3 min  
*d* 4 min

spectrophotometer (LAMBDA 950 Perkin Elmer, USA) in the wavelength range 200–2000 nm.

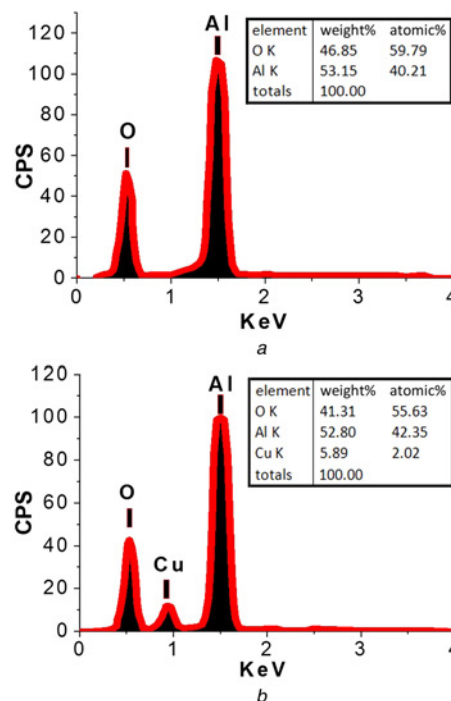


**Fig. 2** EDX spectrum of  
*a* Pure NAAS  
*b* NAAS coated with Cu for 4 min

**3. Results and discussion:** Fig. 1*a* shows a top view FESEM image of a typical NAAS consisting of a highly ordered hexagonal nanoporous arrays formed by the two-step anodisation process. From this figure, the estimated mean values of pore diameter and inter-pore spacing are approximately 61 and 100 nm, respectively.

To explore the effect of deposition time on the morphology of the fabricated Cu films, a series of NAASs were fabricated under the same conditions and sputtered with Cu for different deposition time from 1 to 4 min. For 1 min deposition, Fig. 1*b* indicates that nanoporous ultra-thin Cu layer is deposited only on the top surface of the NAAS and leaves the pores still open. In other words, the obtained Cu films just replicate the NAAS geometry and form an ordered nanoporous structure. This structure gives an opportunity to fabricate Cu nanoporous templates. The mechanism of formation of ordered nanoporous Cu on the top surface of NAAS can be described as follows. During sputtering, Cu ions were electrostatically attracted on the surface of the NAAS by the localised negative charges (anions  $C_2O_4^{2-}$  and  $OH^-$ ) that result in the nucleation of Cu ions on the surface of NAAS rather than in the NAAS channels [19, 20]. By increasing the deposition time to 3 min, more Cu nanoparticles are deposited to generate copper nano-grains and then grew to form a large number of Cu aggregates. Because the deposition rate is very fast, these Cu aggregates are grown rapidly to form continuous layer on the surface of the NAAS. Thus, most of the pores are almost entirely covered with this Cu aggregates (Fig. 1*c*). This layer of Cu aggregates has a rough surface due to the random distribution of the nano-grains. After 4 min deposition, the nucleation and growth of Cu aggregates are increased. These aggregates are coalescent to form continuous layer of large Cu nano-clusters on the surface of the NAAS. These clusters have irregular shapes and sizes leading to rough Cu surface. The nano-clusters have sizes in the range of 25 to 140 nm, as shown in Fig. 1*d*.

The manufactured NAAS and Cu/NAAS were examined by EDX to identify possible impurities in the formation of the Cu and to determine the percentage weight deposition of Cu on the NAASs. Fig. 2*a* shows the EDX pattern of NAAS. There are only signals for Al (53.15%) and O (46.85%), and no traces of

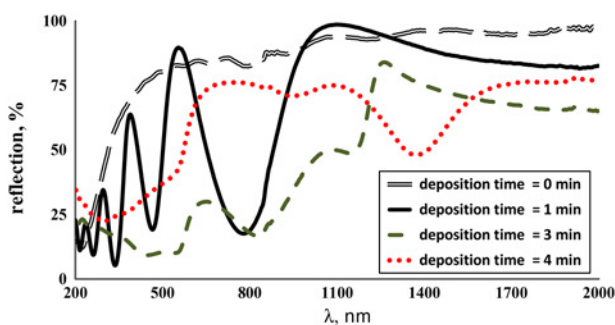


Fig. 3 Reflection spectra of blank and Cu-coated NAASs with various deposition times

elements such as C, Cr or S are detected. This indicates that the NAAS is only pure nanoporous  $\text{Al}_2\text{O}_3$  on the Al substrate.

The EDX pattern in Fig. 2b gives a qualitative analysis, and the inset table provides the quantitative analysis of 4 min-Cu/NAAS sample. As shown a high purity Cu nanostructure is deposited with Cu-deposition weight of 5.89%.

The reflectance spectra of NAAS and Cu/NAAS are shown in Fig. 3. It is clear that the average reflectivity of Cu/NAAS samples is relatively low in the visible region compared with that of the blank NAAS due to the increasing of the absorption as the thickness of Cu layer increased. The reflectance of NAAS is characterised by very small oscillations originates from the interference between the reflected light from the top (air/NAAS) and bottom (NAAS/Al) interfaces. For Cu-coated NAASs, the oscillation strength of the interference fringes is stronger than that of the blank NAAS. The enhancement of the interference fringes is attributed to the strong modulation of light waves reflected from the top interfaces of the nanoporous Cu layer of the coated sample [21]. Consequently, the amplitudes of the reflected rays are enhanced. Therefore, the differences between the minima and maxima of the interference fringes increase.

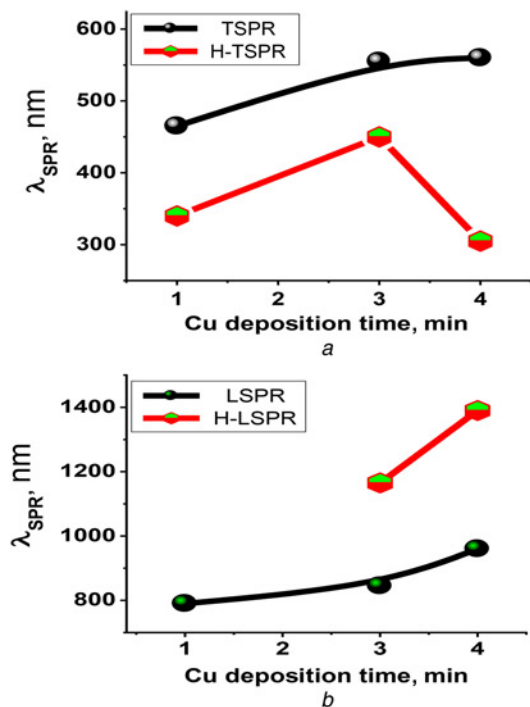


Fig. 4 Resonance wavelength of SPR modes against the deposition time  
a Transverse surface plasmon resonances (TSPRs)  
b Longitudinal surface plasmon resonances (LSPRs)

Moreover, the reflection spectra of Cu/NAAS samples, especially for 1 min coated sample, are characterised by strong and sharp minima assigned to fundamentals and higher-order surface plasmon modes. The SPR position of nanoparticles can be varied by changing their sizes and shapes. For smaller nanoparticles, the electromagnetic field is uniform across the nanoparticle such that all the oscillating electrons move in the same phase and produce only fundamental surface plasmon mode. As the nanoparticle size increases, the induced electric field across the nanoparticle becomes non-uniform, and this phase retardation broadens the dipole resonance and excites higher order resonance modes [22]. After 1 min, Cu-coating, very low reflectivity (5.6%) is observed at 340 nm due to the coupling between the interference mode and the higher-order transverse SPR of the Cu nanoparticles, which leads to a strong and narrow dip in the optical reflection spectra. The broadness of the minimum in the reflection spectrum at 1390 nm for 4 min Cu-coated NAAS most likely originated from the lack of homogeneity in the size and shape of Cu nano-clusters [23]. The important features of SPR modes are summarised in Fig. 4. This figure shows the variation of resonance wavelength (minimum position) with the deposition time of longitudinal surface plasmon resonance (LSPR) and transverse surface plasmon resonance (TSPR) modes.

As shown in Fig. 4a, redshifts of LSPR and higher-order LSPR are observed with increasing the size of Cu nanoparticles. This red shift may be ascribed to the size effect and the coupling effect of surface plasmon interactions. As the particle size increased, the spreading of the particle's surface charge over a larger surface area leads to slow down of the electron oscillations [24]. In addition, the Cu film in our samples consists of a large number of nanoparticles or nano-clusters, as shown Figs. 1c and d, and then the collective contributions to the red-shift are larger than that of an individual nano-cluster due to the coupling of the surface plasmon effects. As shown in Fig. 4b, redshifts of TSPR and higher-order TSPR minima were observed as the size of the Cu nanoparticles increased. After 4 min Cu deposition, the position of the higher-order TSPR was suddenly blue shifted. To understand the origin of this sudden shift, glass slides were coated with Cu nanoparticles at the same conditions. The same behavior was observed for Cu-coated glass slide due to the conversion of Cu film from the individual nanoparticles film to the continuous nanostructured film, which induced the propagating SPR.

**4. Conclusion:** In this work, RF sputtering has been successfully used to deposit ultra-thin nanostructured Cu films of different morphologies on the top surface of NAAS. The morphologies of the Cu nanostructures can be controlled from hexagonal nanoporous Cu array to nanoporous-grains of Cu aggregates, and then to a continuous layer of Cu nanostones by adjusting the sputtering time from 1 to 4 min. According to the study of the optical properties, strong SPRs are obtained at 340, 465, and 790 nm for 1 min Cu-coated sample. The surface plasmon modes are red-shifted to NIR region by increasing the Cu deposition time, which provides a unique opportunity for the design of biological nanodevices.

## 5 References

- [1] Eustis S., El-Sayed M.A.: 'Why gold nanoparticles are more precious than pretty gold: Noble metal surface plasmon resonance and its enhancement of the radiative and nonradiative properties of nanocrystals of different shapes', *Chem. Soc. Rev.*, 2006, **35**, pp. 209–217
- [2] Kai C., Eunice Sok P.L., Michael R., *ET AL.*: 'Active molecular plasmonics: tuning surface plasmon resonances by exploiting molecular dimensions', *Nanophotonics*, 2015, **4**, pp. 186–197
- [3] Jules L.H., Nikhil B., Sarah D.R., *ET AL.*: 'Localized surface plasmon resonance as a biosensing platform for developing countries', *Biosensors*, 2014, **4**, pp. 172–188
- [4] Shaban M., Hamdy H., Shahin F., *ET AL.*: 'Strong surface plasmon resonance of ordered gold nanorod array fabricated in porous anodic alumina template', *J. Nanosci. Nanotechnol.*, 2010, **10**, pp. 3034–3037

- [5] Shaban M., Hamdy H., Shahin F., *ET AL.*: 'Optical properties of porous anodic alumina membrane uniformly decorated with ultra-thin porous gold nanoparticles arrays', *J. Nanosci. Nanotechnol.*, 2011, **11**, pp. 941–952
- [6] Dash P.K., Balto Y.: 'Generation of nano-copper particles through wire explosion method and its characterization', *Res. J. Nanosci. Nanotechnol.*, 2010, **1**, pp. 25–33
- [7] Pei-I W., Sang H.L., Thomas C.P., *ET AL.*: 'Low temperature wafer bonding by copper nanorod array', *Electrochem. Solid-State Lett.*, 2009, **12**, pp. H138–H141
- [8] Eastman J.A., Choi S.U.S., Li S., *ET AL.*: 'Anomalously increased effective thermal conductivities of ethylene glycol-based nanofluids containing copper nanoparticles', *Appl. Phys. Lett.*, 2001, **78**, pp. 718–720
- [9] Wen X., Yutao X., Chun L.C., *ET AL.*: 'Copper-based nanowire materials: templated syntheses, characterizations, and applications', *Langmuir*, 2005, **21**, pp. 4729–4737
- [10] Bjoerksten U., Moser J., Graetzel M.: 'Photoelectrochemical studies on nanocrystalline hematite films', *Chem. Mater.*, 1994, **6**, pp. 858–863
- [11] Jiang Y., Decker S., Mohs C., *ET AL.*: 'Catalytic solid state reactions on the surface of nanoscale metal oxide particles', *J. Catal.*, 1998, **180**, pp. 24–35
- [12] Changjiang Z., Xi J., Lini Y., *ET AL.*: 'Low temperature carbon monoxide oxidation with Au-Cu meatball-like cages prepared by galvanic replacement', *Chem. Sus. Chem.*, 2013, **6**, pp. 1883–1887
- [13] Duan J.L., Cornelius T.W., Liu J., *ET AL.*: 'Surface plasmon resonances of Cu nanowire arrays', *J. Phys. Chem. C*, 2009, **113**, pp. 13583–13587
- [14] George H.C., Zhao J., Hicks E.M., *ET AL.*: 'Plasmonic properties of copper nanoparticles fabricated by nanosphere lithography', *Nano Lett.*, 2007, **7**, pp. 1947–1952
- [15] Park S.K., Noh J.S., Chin W.B., *ET AL.*: 'Fabrication of metal nanodot arrays using a porous alumina membrane as a template', *Curr. Appl. Phys.*, 2007, **7**, pp. 180–185
- [16] Yaya Z., Xu W., Xu S., *ET AL.*: 'Optical properties of Ni and Cu nanowire arrays and Ni/Cu superlattice nanowire arrays', *Nanoscale Res. Lett.*, 2012, **7**, p. 569
- [17] Shaban M., Hamdy H., Shahin F., *ET AL.*: 'Uniform and reproducible barrier layer removal of porous anodic alumina membrane', *J. Nanosci. Nanotechnol.*, 2010, **10**, pp. 3380–3384
- [18] Shaban M., Ali M., Abdelhady K., *ET AL.*: 'Al<sub>2</sub>O<sub>3</sub> and Sn/Al<sub>2</sub>O<sub>3</sub> nanowires: fabrication and characterization', *Micro Nano Lett.*, 2015, **10**, (7), p. 324
- [19] Choi J., Luo Y., Wehrspohn R.B., *ET AL.*: 'Perfect two-dimensional porous alumina photonic crystals with duplex oxide layers', *J. Appl. Phys.*, 2003, **94**, pp. 4757–4762
- [20] Ling Z., Chen S., Wang J., *ET AL.*: 'Fabrication and properties of anodic alumina humidity sensor with through-hole structure', *Chin. Sci. Bull.*, 2008, **53**, pp. 183–187
- [21] Ji N., Ruan W., Wang C., *ET AL.*: 'Fabrication of silver decorated anodic aluminum oxide substrate and its optical properties on surface-enhanced Raman scattering and thin film interference', *Langmuir*, 2009, **25**, pp. 11869–11873
- [22] Evanoff Jr. D.D., Chumanov G.: 'Synthesis and optical properties of silver nanoparticles and arrays', *Chem. Phys. Chem.*, 2005, **7**, pp. 1221–1231
- [23] Chen H., Lee J.H., Kim Y.H., *ET AL.*: 'Metallic copper nanostructures synthesized by a facile hydrothermal method', *J. Nanosci. Nanotechnol.*, 2010, **10**, pp. 629–636
- [24] Kreibig U., Vollmer M.: 'Optical properties of metal clusters', Springer Series in Materials Science, Springer-Verlag, New York, 1995